

# Electric Vehicle Charging Load Forecasting: An Experimental Comparison of Machine Learning Methods

Iason Kyriakopoulos  
University of Piraeus, Greece  
iasonkyriakop@gmail.com

Yannis Theodoridis  
University of Piraeus, Greece  
ytheod@unipi.gr

December 22, 2025

## Abstract

With the growing popularity of electric vehicles as a means of addressing climate change, concerns have emerged regarding their impact on electric grid management. As a result, predicting EV charging demand has become a timely and important research problem. While substantial research has addressed energy load forecasting in transportation, relatively few studies systematically compare multiple forecasting methods across different temporal horizons and spatial aggregation levels in diverse urban settings. This work investigates the effectiveness of five time series forecasting models, ranging from traditional statistical approaches to machine learning and deep learning methods. Forecasting performance is evaluated for short-, mid-, and long-term horizons (on the order of minutes, hours, and days, respectively), and across spatial scales ranging from individual charging stations to regional and city-level aggregations. The analysis is conducted on four publicly available real-world datasets, with results reported independently for each dataset. The results show that forecasting performance varies substantially across models, forecasting horizons, and spatial aggregation levels. Transformer models demonstrate strong performance in short-term forecasting, particularly at regional and city aggregation levels, while LSTM exhibits pronounced dataset-specific dominance in certain cases. For mid- and long-term forecasting, recurrent neural networks, especially GRU and LSTM, consistently achieve the lowest errors across most datasets and aggregation levels, highlighting their ability to model complex sequential dependencies. Transformer models perform competitively but display sensitivity to dataset characteristics, whereas ARIMA and XGBoost are competitive only in localized scenarios and do not scale reliably to longer horizons or higher aggregation levels. To the best of our knowledge, this is the first work to systematically evaluate EV charging demand forecasting across such a wide range of temporal horizons and spatial aggregation levels using multiple real-world datasets.

## 1 Introduction

Electric Vehicles (EVs) have emerged as a key solution to mitigating climate change by reducing greenhouse gas emissions and fossil fuel dependence, thereby supporting the transition toward more sustainable transportation systems [1]. Their global adoption is rapidly accelerating, driven by international policies, such as the Paris Agreement [2], which sets legally binding carbon neutrality targets and promotes the electrification of transport. As the number of EVs grows, so does electricity demand, creating challenges for grid management, energy planning, and infrastructure development. Forecasting consumption, ranging from individual stations to city-wide levels, is essential for ensuring a reliable energy supply [3], preventing overloads, and enabling the integration

of renewable sources. Accurate forecasts also contribute to grid stability by anticipating load fluctuations, optimizing the allocation of charging infrastructure, and inform energy and urban planning policies, making them fundamental for the development of smarter and cleaner cities [4].

Despite its importance, forecasting EV charging consumption remains a complex and demanding task [5]. The challenges stem from both data limitations and the inherent irregularity of EV usage patterns, as well as from methodological and evaluation issues. A central obstacle is the scarcity of open-source EV charging datasets [6], with existing data varying widely in structure and scope, thereby complicating benchmarking and model comparison. Furthermore, charging events occur irregularly, particularly at the station level, making traditional time series forecasting methods less effective. External drivers, such as electricity prices, weather conditions, traffic, and other contextual factors, strongly influence charging demand [7], yet are difficult to incorporate comprehensively into forecasting models. Consumption also displays layered temporal patterns and seasonality [8], including daily (e.g., peak hours, daytime vs. night), weekly (e.g., weekday vs. weekend), and yearly (e.g., winter vs. summer) cycles, which require models capable of capturing such overlapping dynamics. Additionally, the rapid growth in EV adoption continuously reshapes usage patterns, necessitating forecasting approaches that can adapt to evolving trends. Finally, predictions are required at different levels of aggregation, from single stations to entire cities, each presenting distinct patterns and challenges that call for flexible and scalable modeling frameworks.

The main objective of this research is therefore to conduct a systematic comparison of several state-of-the-art forecasting models applied to EV charging consumption data. The study evaluates how these models perform across different temporal resolutions, with the goal of drawing meaningful conclusions about their applicability, strengths, and limitations in this domain.

To this end, the research focuses on forecasting EV charging consumption using five models, ranging from classical statistical approaches (ARIMA) to machine learning (XGBoost) and deep learning (GRU, LSTM, Transformer) methods. These models are trained on four popular real-world EV charging datasets from four cities (namely, Palo Alto, Boulder, Dundee, and Perth) at multiple aggregation levels spanning individual charging stations to regional and city-wide consumption. The comparison is performed across several forecasting horizons: short-term (up to 30 minutes ahead, in 10-minute steps), mid-term (up to 8 hours ahead, in 2-hour steps), and long-term (up to 5 days ahead, in 1-day steps).

The remainder of the paper is organized as follows. Section II formalizes the EV charging load forecasting problem and outlines the forecasting methods considered. Section III presents the datasets, the preprocessing pipeline, and the performance evaluation framework. Section IV describes the experimental setup and reports the results with comparative analysis and discussion. Section V reviews directly comparable related work. Section VI concludes and outlines directions for future research.<sup>1</sup>

---

<sup>1</sup>For reproducibility purposes, the entire experimental protocol (data preprocessing, model training, inference, and evaluation pipelines), together with links to datasets, is available at <https://github.com/DataStories-UniPi/electric-vehicle-charging-load-forecasting>.

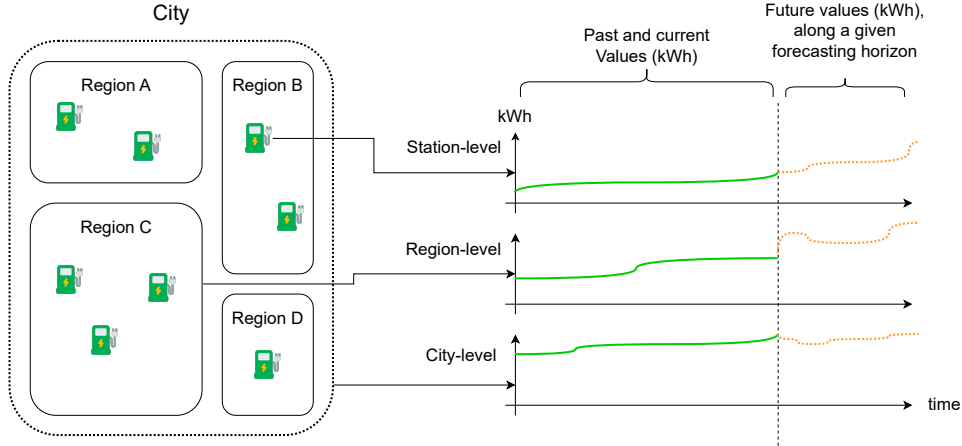


Figure 1: Illustration of the EV charging load forecasting problem.

## 2 THE EV CHARGING LOAD FORECASTING PROBLEM AND RELATED METHODS

### 2.1 PROBLEM DEFINITION IN TERMS OF TIME SERIES FORECASTING

The primary task of this study is to forecast the total energy consumption (in kWh) of EV charging infrastructure over future time intervals. Formally, the problem at hand is formulated as follows:

**The EV Charging Load Forecasting Problem:** Given a historical sequence of aggregated charging energy consumption values

$$X = \{x_1, x_2, \dots, x_T\},$$

where  $x_t$  represents the total energy consumed at time step  $t$ , the objective is to train a model that can predict future consumption values

$$\hat{X} = \{\hat{x}_{T+1}, \hat{x}_{T+2}, \dots, \hat{x}_{T+H}\},$$

over a forecasting horizon  $H$ . Depending on the application,  $H$  could correspond to short- (order of minutes), mid- (order of hours), or long-term (order of days) predictions. These horizons enable the evaluation of forecasting models under varying temporal complexities, ranging from near real-time operational to strategic planning decisions.

As inferred by the problem definition above, forecasting can be conducted at multiple spatial aggregation levels. At the charging station level, each individual station is treated as a separate time series. At the regional level, groups of stations within a given area are combined, and their total energy consumption aggregated to reflect regional demand. At the city level, all stations within a city are aggregated into a single time series representing overall city-wide load. The aforementioned discussion is illustrated in Fig. 1.

By combining multiple prediction horizons with different spatial resolutions, this study establishes a multi-scale forecasting framework. This framework enables systematic evaluation of model performance across fine-grained local scales and broader aggregated levels, while also accounting for short-term fluctuations and longer-term trends.

## 2.2 STATE-OF-THE-ART MACHINE LEARNING METHODS

As already mentioned, this study compares forecasting models spanning traditional statistical approaches, machine learning, and deep learning. The selection balances established baselines with state-of-the-art methods well-suited for time series forecasting in the context of EV consumption.

ARIMA (Autoregressive Integrated Moving Average) serves as a baseline due to its simplicity, interpretability, and long-standing use in time series analysis [9]. XGBoost (Extreme Gradient Boosting) is a tree-based ensemble method capable of efficiently modeling non-linear relationships, providing a strong benchmark against both statistical and deep learning approaches [10]. Gated Recurrent Units (GRU) are recurrent neural networks designed to handle sequential data through gating mechanisms, mitigating vanishing gradient issues and capturing medium- to long-term dependencies [11]. Long Short-Term Memory (LSTM) networks extend traditional RNNs with memory cells and gating mechanisms, enabling the modeling of long-range temporal dependencies, and remain widely used in time series forecasting as a robust deep learning architecture [12]. Based on self-attention mechanisms, Transformers can capture dependencies across entire sequences in parallel and are increasingly applied in time series forecasting [13].

Prior research highlights the strengths and limitations of these forecasting approaches. However, through the detailed overview of related work that is presented in Section V, it turns out that, despite continuous progress in EV load forecasting research, notable gaps remain. Few studies systematically evaluate how models trained at the station level scale to regional or city-level consumption, leaving open questions about multi-scale adaptability. Moreover, many works assess performance at a single forecast horizon, and standardized comparisons across short-, mid-, and long-term horizons are rare. This study primarily addresses these two challenges: (i) scalability across different spatial levels (from individual stations to city-wide aggregation) and (ii) systematic performance comparison across multiple forecasting horizons.

## 3 THE EXPERIMENTAL COMPARISON FRAMEWORK

This section outlines the experimental framework used to compare forecasting models under consistent conditions. It describes how real-world EV charging datasets are standardized and transformed into time series suitable for model training, and how model performance is evaluated across multiple spatial aggregation levels and temporal horizons. The framework ensures methodological uniformity, enabling meaningful comparison of statistical, machine learning, and deep learning approaches. A bird’s-eye view of the framework architecture is illustrated in Fig. 2.

### 3.1 Datasets and Preprocessing

This study utilizes four popular real-world datasets of EV charging sessions collected from different cities, namely, Palo Alto, Boulder, Dundee, and Perth [14]. Each dataset contains individual charging sessions, with varying duration, spatial coverage, granularity, and associated metadata. Table 1 provides an overview of the dataset characteristics. To ensure consistency and comparability across the diverse datasets, a unified preprocessing pipeline has been developed and applied to all of them, as it is described in the paragraphs that follow.

Each dataset originally contained a mix of core and auxiliary fields. The columns retained across all cities included the start and end times of each charging session (merged from separate date and time fields when necessary), energy consumption in kWh per session, a station identifier, and a regional grouping field (e.g., ZIP code or site label). Auxiliary fields that were either irrelevant for

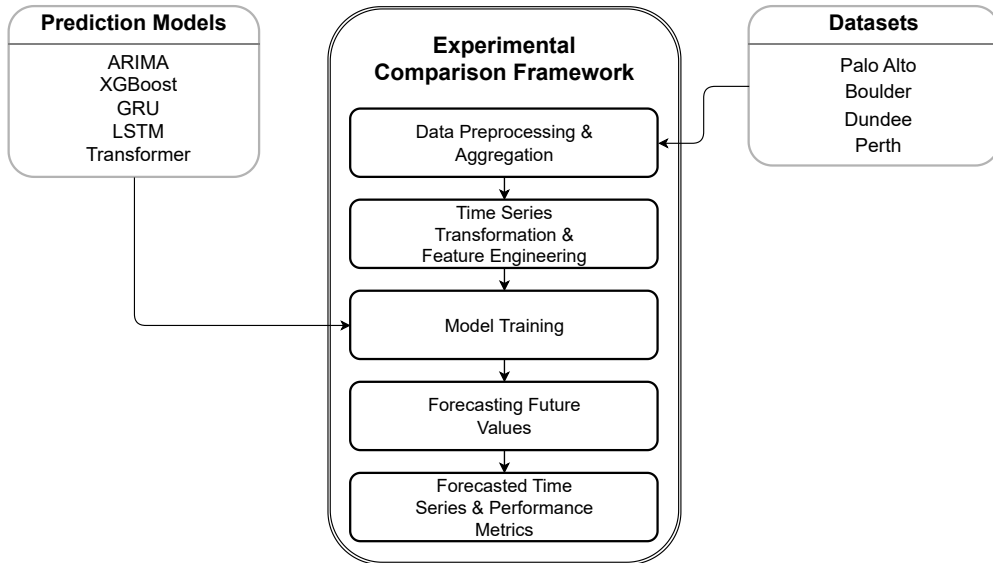


Figure 2: Overview of the experimental comparison framework.

Table 1: Overview of EV Charging Datasets

City	Time Range	Nr. of Stations	Nr. of Regions	Nr. of Charging Session Records
Palo Alto, CA (USA)	July 2011 – Dec. 2020	47	3	259,415
Boulder, CO (USA)	Jan. 2018 – Mar. 2021	27	5	24,081
Dundee (UK)	Jan. 2017 – Dec. 2018	67	34	52,752
Perth (Australia)	Jan. 2016 – Dec. 2019	36	22	66,664

forecasting or inconsistently available, such as port type, greenhouse gas emissions saved, session ID, and user ID, were excluded.

A small fraction of missing values was present. To maintain simplicity and avoid introducing assumptions, rows with missing entries were removed, resulting in minimal data loss. Data integrity checks were also performed to exclude invalid sessions for the purpose of our study, such as those reporting negative energy consumption or end times preceding start times.

Time zones were standardized for consistency. Datasets with timezone-aware timestamps were converted to Coordinated Universal Time (UTC), while datasets lacking explicit timezone metadata were assumed to follow the local time of the respective city.

To transform session-based data into a time series format, energy consumption was aggregated into fixed 10-minute intervals per station by summing energy from all sessions overlapping each interval. This 10-minute resolution served as the base granularity, from which hourly and daily time series were derived through resampling.

Additional time-based features were engineered, including calendar variables such as holidays,

weekends, day of the week, and month of the year. To capture temporal dependencies, multiple lagged versions of the target variable were generated at different offsets appropriate to each temporal resolution (10-minute, hourly, and daily). This ensured that both short-term fluctuations and longer-term seasonal patterns were represented in the feature space.

Finally, energy consumption values were normalized using the standard z-score normalization. Forecasts were evaluated directly in the normalized domain, without inverse transformation, to enable consistent comparison across datasets and with prior studies (see Section V).

### 3.2 THE PERFORMANCE EVALUATION PROTOCOL

To ensure a fair and consistent comparison, a unified evaluation protocol is applied. Each model is evaluated across all short-, mid-, and long-term forecasting horizons and across all spatial aggregation levels (station, region, and city). Evaluation is performed independently for each dataset, producing one set of performance scores per dataset for every combination of forecasting horizon and spatial aggregation level. Results are reported per dataset, with the best-performing model highlighted for each combination of dataset, spatial aggregation level, forecasting horizon, and error metric.

Performance is assessed using two standard error metrics, namely, MAE, which provides an intuitive measure of average error magnitude, and RMSE, which penalizes larger errors more strongly and is therefore sensitive to outliers. These two metrics were selected for their simplicity, interpretability, and widespread use in time series forecasting literature [7]. Other metrics such as MAPE were avoided due to instability when actual values approach zero [15], while  $R^2$  was excluded as it is less interpretable in non-linear forecasting contexts [16].

## 4 EXPERIMENTAL STUDY

### 4.1 EXPERIMENTAL SETUP

This section outlines the technical environment and modeling configurations used in the experimental process.

Two distinct modeling strategies were adopted in this study. The first strategy employed multi-station learning, where a single model was trained per city and temporal resolution using pooled data from all stations. This approach was applied to XGBoost, GRU, LSTM, and Transformer architectures. The input space combined one-hot encodings of station and region identifiers with calendar and holiday indicators. All lagged features and target values were standardized using z-score normalization computed from the training partition. Forecasting was conducted in a recursive walk-forward manner, where predictions at each step were iteratively fed back as inputs, thereby updating the lag state of each station over time.

The second strategy relied on per-station univariate ARIMA modeling. Here, each charging station was treated independently, and ARIMA models were fitted to standardized series of energy consumption. To constrain computational cost, order selection was performed using a restricted grid search over  $(p, d, q)$  with  $p, q \in \{0, 1, 2\}$  and  $d \in \{0, 1\}$ , selecting the specification with the lowest AIC (Akaike Information Criterion). Training was limited to a capped recent window of the data 2,048 points for 10-minute, 1,536 for hourly, and 730 for daily resolution (corresponding roughly to two weeks, two months, and two years of history, respectively), which balances computational feasibility with the amount of recent information typically sufficient for reliable ARIMA estimation. Stationarity and invertibility were enforced, and when estimation failed, a naïve persistence model was substituted.

All models were trained and evaluated over three temporal resolutions:

- **Short-term forecasting:** 10 up to 30 minutes, in steps of 10 minutes (i.e., 3 steps);
- **Mid-term forecasting:** 2 up to 8 hours, in steps of 2 hours (i.e., 4 steps); and
- **Long-term forecasting:** 1 up to 5 days, in steps of 1 day (i.e., 5 steps).

Hyperparameters for the learning models were fixed rather than exhaustively tuned, in order to ensure reproducibility and maintain computational feasibility across datasets. GPU acceleration was used for XGBoost and neural models, while ARIMA was executed on CPU. The settings were as follows:

- **ARIMA:** per-station order selected from the restricted AIC grid as described above, trained on the capped tail of the training set, and used to forecast the full test horizon.
- **XGBoost:** `device=cuda`, `tree_method=hist`; learning rate 0.05; maximum depth 8; subsample 0.8; `colsample_bytree` 0.8;  $\ell_2$  regularization 1.0; up to 2000 rounds with early stopping (patience 200).
- **GRU/LSTM:** sequence length equal to the number of engineered lag features; 64 hidden units; Adam optimizer ( $10^{-3}$ ); batch size 2048; maximum 200 epochs with early stopping (patience 20); TensorFlow mixed precision enabled on GPU.
- **Transformer:**  $d_{\text{model}}=128$ , 8 attention heads, 4 layers, feed-forward dimension 256, dropout 0.1; trained with the same optimizer, batch size, early stopping, and mixed precision settings, as with GRU/LSTM.

All experiments were conducted in Python, with version 3.10 used for data preprocessing and version 3.8 for forecasting, model training and inference. The models were developed using standard open-source libraries, including `pandas`, `numpy`, `statsmodels`, `scikit-learn`, and `tensorflow`.

Model training and evaluation were performed on a single NVIDIA A100 GPU node with 1 TB of system memory. Leveraging GPU acceleration significantly reduced training times for deep learning models, enabling efficient experimentation across all datasets.

## 4.2 EXPERIMENTAL RESULTS

In the following paragraphs, we present the performance of each of the five models across the different forecasting horizons and spatial aggregation levels.

Tables 2–4 summarize model performance for short-, mid-, and long-term horizons at different spatial aggregation levels and for each dataset. In particular, Table 2 presents short-term (10-30 minutes) results, Table 3 shows mid-term (2-8 hours) outcomes, and Table 4 reports long-term (1-5 days) forecasting accuracy. Each table includes results at the station, regional, and city levels, with the best-performing model highlighted in bold for each metric and aggregation level combination.

For short-term forecasting (up to 30 minutes, in 10-minute steps, as reported in Table 2), performance exhibits clear dataset-dependent behavior. In the Perth dataset, LSTM consistently achieves the lowest errors across all spatial aggregation levels and horizons, dominating station-, regional-, and city-level forecasts. For example, at the station level, LSTM attains MAE values between 0.43 and 0.46 and RMSE values below 1.1 across all short-term horizons, substantially outperforming competing models. In the remaining datasets, Transformer models demonstrate the strongest overall performance. In Boulder, Transformers achieve the lowest MAE across all spatial levels and

Table 2: Forecasting results for up to 30-minute horizon (10-minute steps). Datasets: Palo Alto, Boulder, Dundee, Perth. Lower is better.

Model	Dataset	Metric	10 minutes			20 minutes			30 minutes		
			Station	Region	City	Station	Region	City	Station	Region	City
ARIMA	Palo Alto	MAE	0.92	6.34	13.12	0.91	6.33	13.09	0.91	6.31	13.06
		RMSE	1.19	8.14	15.54	1.18	8.11	15.49	1.17	8.09	15.45
	Boulder	MAE	0.26	0.85	3.11	0.26	0.84	3.06	0.26	0.83	3.04
		RMSE	0.68	<b>1.50</b>	4.14	<b>0.66</b>	<b>1.47</b>	4.08	<b>0.65</b>	<b>1.45</b>	4.04
	Dundee	MAE	<b>0.62</b>	1.26	18.16	<b>0.61</b>	1.25	17.58	<b>0.61</b>	1.25	17.30
		RMSE	1.43	2.19	23.81	1.28	2.05	22.66	1.20	1.97	21.99
	Perth	MAE	0.62	1.60	12.02	0.61	1.59	11.62	0.61	1.58	11.37
		RMSE	1.36	2.91	13.78	1.26	2.72	13.18	1.20	2.61	12.83
XGBoost	Palo Alto	MAE	<b>0.88</b>	5.67	14.71	<b>0.87</b>	5.64	14.67	<b>0.87</b>	5.62	14.64
		RMSE	<b>1.02</b>	6.38	16.28	<b>1.01</b>	6.35	16.24	<b>1.00</b>	6.32	16.20
	Boulder	MAE	0.87	3.29	14.80	0.86	3.28	14.80	0.86	3.26	14.79
		RMSE	0.98	3.47	15.52	0.96	3.45	15.50	0.96	3.44	15.49
	Dundee	MAE	1.37	2.69	55.99	1.31	2.61	55.80	1.26	2.57	55.70
		RMSE	1.67	2.97	58.80	1.56	2.88	58.40	1.49	2.82	58.16
	Perth	MAE	0.94	2.27	21.52	0.91	2.20	21.12	0.90	2.14	20.88
		RMSE	1.36	2.81	23.33	1.26	2.64	23.00	1.20	2.54	22.81
GRU	Palo Alto	MAE	1.05	6.07	16.55	1.04	6.04	16.51	1.04	6.02	16.48
		RMSE	1.15	6.72	18.14	1.13	6.69	18.10	1.13	6.67	18.07
	Boulder	MAE	0.32	0.97	2.81	0.31	0.95	2.76	0.31	0.94	2.72
		RMSE	0.68	1.59	<b>4.09</b>	0.67	1.55	<b>4.02</b>	<b>0.65</b>	1.53	<b>3.97</b>
	Dundee	MAE	1.08	1.89	33.22	1.03	1.81	32.75	0.99	1.76	32.48
		RMSE	1.45	2.25	35.60	1.33	2.13	34.95	1.25	2.06	34.56
	Perth	MAE	0.85	2.03	17.67	0.83	1.95	17.39	0.81	1.90	17.24
		RMSE	1.43	2.88	20.54	1.33	2.71	20.17	1.27	2.61	19.95
LSTM	Palo Alto	MAE	1.00	5.87	15.87	0.99	5.85	15.84	0.98	5.83	15.81
		RMSE	1.10	6.53	17.46	1.09	6.50	17.42	1.08	6.47	17.38
	Boulder	MAE	0.54	1.90	7.11	0.53	1.89	7.07	0.53	1.88	7.04
		RMSE	0.91	2.57	8.70	0.90	2.55	8.67	0.89	2.53	8.64
	Dundee	MAE	1.49	2.89	64.93	1.44	2.81	64.78	1.40	2.75	64.69
		RMSE	1.85	3.20	68.71	1.72	3.09	68.36	1.65	3.02	68.14
	Perth	MAE	<b>0.46</b>	<b>1.07</b>	<b>7.97</b>	<b>0.44</b>	<b>1.03</b>	<b>7.54</b>	<b>0.43</b>	<b>0.99</b>	<b>7.27</b>
		RMSE	<b>1.06</b>	<b>2.09</b>	<b>10.98</b>	<b>0.95</b>	<b>1.88</b>	<b>10.27</b>	<b>0.88</b>	<b>1.74</b>	<b>9.84</b>
Transformer	Palo Alto	MAE	0.93	<b>5.17</b>	<b>12.84</b>	0.92	<b>5.15</b>	<b>12.80</b>	0.91	<b>5.13</b>	<b>12.77</b>
		RMSE	1.11	<b>5.98</b>	<b>14.34</b>	1.10	<b>5.94</b>	<b>14.29</b>	1.09	<b>5.91</b>	<b>14.25</b>
	Boulder	MAE	<b>0.22</b>	<b>0.76</b>	<b>2.71</b>	<b>0.21</b>	<b>0.76</b>	<b>2.67</b>	<b>0.21</b>	<b>0.75</b>	<b>2.65</b>
		RMSE	<b>0.67</b>	1.58	4.34	<b>0.66</b>	1.54	4.27	<b>0.65</b>	1.52	4.22
	Dundee	MAE	0.73	<b>1.17</b>	<b>14.52</b>	0.68	<b>1.09</b>	<b>13.70</b>	0.63	<b>1.04</b>	<b>13.22</b>
		RMSE	<b>1.18</b>	<b>1.70</b>	<b>18.54</b>	<b>1.04</b>	<b>1.56</b>	<b>17.22</b>	<b>0.95</b>	<b>1.46</b>	<b>16.43</b>
	Perth	MAE	1.53	3.79	42.94	1.49	3.70	42.91	1.46	3.65	42.90
		RMSE	1.89	4.30	45.40	1.81	4.18	45.23	1.77	4.10	45.13

Table 3: Forecasting results for up to 8-hour horizon (2-hour steps). Datasets: Palo Alto, Boulder, Dundee, Perth. Lower is better.

Model	Dataset	Metric	2 hours			4 hours			6 hours			8 hours		
			St.	Reg.	City									
ARIMA	Palo Alto	MAE	0.74	5.10	13.30	0.72	4.92	12.81	0.70	4.71	12.50	0.69	4.49	11.21
		RMSE	1.00	6.90	17.35	0.96	6.66	16.90	0.91	6.47	16.57	0.87	6.14	15.55
	Boulder	MAE	<b>0.28</b>	<b>0.85</b>	3.08	<b>0.27</b>	<b>0.79</b>	2.83	<b>0.27</b>	<b>0.75</b>	2.68	<b>0.26</b>	<b>0.72</b>	2.42
		RMSE	<b>0.63</b>	<b>1.43</b>	4.08	<b>0.56</b>	<b>1.27</b>	3.73	<b>0.51</b>	<b>1.16</b>	3.43	0.47	<b>1.08</b>	3.24
	Dundee	MAE	1.09	1.91	31.66	1.07	1.86	30.77	1.06	1.84	30.23	1.06	1.83	29.88
		RMSE	1.53	2.42	36.00	1.43	2.32	35.28	1.38	2.25	34.88	1.34	2.21	34.60
	Perth	MAE	0.93	2.18	19.02	0.90	2.07	18.25	0.88	2.01	17.22	0.86	1.98	16.50
		RMSE	1.35	2.83	21.34	1.22	2.59	20.68	1.14	2.44	19.82	1.10	2.36	19.22
XGBoost	Palo Alto	MAE	0.59	3.22	7.81	0.45	2.98	7.40	0.42	2.84	7.16	<b>0.39</b>	2.67	6.82
		RMSE	<b>0.74</b>	3.93	9.28	<b>0.60</b>	3.59	8.75	<b>0.54</b>	3.41	8.46	<b>0.49</b>	3.20	8.09
	Boulder	MAE	0.57	1.92	7.80	0.54	1.84	7.74	0.51	1.78	7.69	0.49	1.75	7.67
		RMSE	0.75	2.22	8.43	0.68	2.09	8.27	0.63	1.99	8.12	0.58	1.94	8.08
	Dundee	MAE	1.16	2.40	53.64	1.08	2.30	53.44	1.05	2.26	53.51	1.02	2.23	53.46
		RMSE	1.38	2.70	56.18	1.26	2.57	55.82	1.20	2.50	55.58	1.17	2.46	55.50
	Perth	MAE	0.63	1.42	11.73	0.56	1.26	10.96	0.51	1.16	10.16	0.49	1.10	10.09
		RMSE	0.94	1.89	13.80	0.78	1.60	13.02	0.69	1.43	12.33	0.64	1.35	12.16
GRU	Palo Alto	MAE	0.63	3.63	9.01	0.54	3.36	8.48	0.50	3.20	8.23	0.47	3.05	7.95
		RMSE	0.79	4.76	11.99	0.70	4.43	11.45	0.63	4.15	10.84	0.58	3.85	10.13
	Boulder	MAE	0.70	2.52	11.03	0.67	2.43	10.97	0.65	2.37	10.94	0.62	2.33	10.93
		RMSE	0.96	3.07	12.01	0.90	2.95	11.82	0.84	2.84	11.74	0.79	2.78	11.67
	Dundee	MAE	<b>0.78</b>	<b>1.36</b>	<b>20.36</b>	<b>0.69</b>	<b>1.26</b>	<b>19.61</b>	<b>0.65</b>	<b>1.20</b>	<b>19.03</b>	<b>0.62</b>	<b>1.17</b>	<b>18.91</b>
		RMSE	<b>1.03</b>	<b>1.75</b>	<b>23.23</b>	<b>0.90</b>	<b>1.60</b>	<b>22.21</b>	<b>0.83</b>	<b>1.50</b>	<b>21.46</b>	<b>0.79</b>	<b>1.46</b>	<b>21.30</b>
	Perth	MAE	<b>0.53</b>	<b>1.17</b>	<b>8.17</b>	<b>0.47</b>	<b>1.03</b>	<b>7.43</b>	<b>0.43</b>	<b>0.94</b>	<b>6.76</b>	<b>0.41</b>	<b>0.89</b>	<b>6.54</b>
		RMSE	<b>0.92</b>	<b>1.83</b>	<b>11.74</b>	<b>0.75</b>	<b>1.52</b>	<b>10.82</b>	<b>0.65</b>	<b>1.34</b>	<b>10.02</b>	<b>0.60</b>	<b>1.24</b>	<b>9.67</b>
LSTM	Palo Alto	MAE	0.63	3.32	8.13	0.51	3.06	7.61	0.47	2.92	7.34	0.44	2.79	7.08
		RMSE	0.79	4.21	10.00	0.65	3.86	9.37	0.59	3.65	8.99	0.55	3.44	8.61
	Boulder	MAE	0.37	1.07	<b>2.91</b>	0.35	0.99	<b>2.64</b>	0.34	0.95	<b>2.46</b>	0.31	0.90	<b>2.39</b>
		RMSE	0.69	1.62	<b>3.95</b>	0.62	1.46	<b>3.54</b>	0.56	1.33	<b>3.15</b>	0.50	1.25	<b>3.07</b>
	Dundee	MAE	1.05	2.02	40.20	0.97	1.93	39.90	0.93	1.89	39.66	0.91	1.85	39.66
		RMSE	1.32	2.44	43.48	1.20	2.31	43.02	1.15	2.24	42.76	1.10	2.19	42.56
	Perth	MAE	0.61	1.39	10.25	0.54	1.24	9.49	0.50	1.14	8.71	0.48	1.08	8.60
		RMSE	0.97	1.97	13.25	0.81	1.67	12.46	0.71	1.50	11.79	0.66	1.41	11.52
Transformer	Palo Alto	MAE	<b>0.56</b>	<b>2.72</b>	<b>6.02</b>	<b>0.44</b>	<b>2.45</b>	<b>5.46</b>	<b>0.41</b>	<b>2.29</b>	<b>5.17</b>	<b>0.39</b>	<b>2.17</b>	<b>4.99</b>
		RMSE	0.76	<b>3.68</b>	<b>8.07</b>	0.62	<b>3.27</b>	<b>7.27</b>	0.56	<b>3.02</b>	<b>6.79</b>	0.51	<b>2.78</b>	<b>6.33</b>
	Boulder	MAE	0.33	0.99	3.06	0.31	0.91	2.78	0.30	0.86	2.60	0.27	0.81	2.51
		RMSE	0.66	1.60	4.52	0.58	1.40	3.93	0.52	1.26	3.57	<b>0.46</b>	1.18	3.43
	Dundee	MAE	1.07	2.12	41.31	0.99	2.05	41.02	0.96	2.02	40.99	0.93	2.00	40.81
		RMSE	1.34	2.52	44.27	1.23	2.41	43.73	1.17	2.36	43.53	1.13	2.31	43.12
	Perth	MAE	0.71	1.64	13.72	0.64	1.47	12.89	0.60	1.36	12.16	0.57	1.32	11.94
		RMSE	0.99	2.07	16.31	0.84	1.79	15.64	0.75	1.63	15.02	0.71	1.55	14.85

Table 4: Forecasting results for up to 5-day horizon (1-day steps). Datasets: Palo Alto, Boulder, Dundee, Perth. Lower is better.

Model	Dataset	Metric	1 day			2 days			3 days			4 days			5 days		
			St.	Reg.	City												
ARIMA	Palo Alto	MAE	0.88	5.15	13.43	0.79	4.78	12.74	0.77	4.54	12.14	0.75	4.32	11.69	0.75	4.21	11.43
		RMSE	1.00	6.43	17.33	0.91	6.06	16.74	0.87	5.86	16.34	0.85	5.70	16.07	0.84	5.61	15.87
	Boulder	MAE	0.84	3.17	13.46	0.78	3.05	13.39	0.76	3.02	13.46	0.75	2.98	13.38	0.74	2.97	13.42
		RMSE	0.99	3.42	14.05	0.89	3.27	13.94	0.85	3.19	13.89	0.83	3.15	13.83	0.81	3.14	13.85
	Dundee	MAE	1.06	2.13	33.22	1.03	2.08	32.45	1.02	2.07	32.25	1.00	2.04	31.47	1.00	2.04	30.93
		RMSE	1.25	2.48	41.59	1.20	2.42	40.82	1.17	2.37	40.29	1.14	2.32	39.71	1.13	2.32	39.82
	Perth	MAE	0.98	2.14	20.09	0.91	1.99	18.96	0.88	1.91	18.35	0.86	1.85	17.53	0.84	1.80	16.62
		RMSE	1.27	2.63	<b>22.00</b>	1.13	2.39	<b>20.90</b>	1.07	2.28	<b>20.20</b>	1.03	2.19	<b>19.40</b>	0.99	2.12	<b>18.60</b>
XGBoost	Palo Alto	MAE	0.75	6.10	17.29	0.76	5.94	17.17	0.74	5.86	17.11	0.72	5.83	17.12	0.72	5.81	17.08
		RMSE	0.87	7.61	21.51	0.89	7.43	21.25	0.86	7.32	21.07	0.83	7.28	21.01	0.82	7.24	20.92
	Boulder	MAE	0.70	2.28	9.42	0.60	2.12	9.35	0.54	2.05	9.39	0.53	2.02	9.43	0.51	2.00	9.36
		RMSE	0.81	2.52	10.15	0.67	2.31	9.87	0.60	2.21	9.74	0.59	2.16	9.71	0.56	2.13	9.63
	Dundee	MAE	0.88	2.17	36.83	0.85	2.12	36.78	0.83	2.09	35.56	0.82	2.06	35.15	0.82	2.07	35.79
		RMSE	1.07	2.42	40.85	1.01	2.35	40.19	0.96	2.26	39.50	0.94	2.23	38.46	0.94	2.22	39.06
	Perth	MAE	0.91	2.02	19.36	0.78	1.76	18.02	0.72	1.63	17.25	0.68	1.56	16.79	0.62	1.42	15.53
		RMSE	1.10	<b>2.38</b>	23.58	0.93	<b>2.10</b>	22.33	0.85	<b>1.97</b>	21.43	0.81	<b>1.90</b>	21.05	0.75	<b>1.76</b>	19.51
GRU	Palo Alto	MAE	0.57	4.93	13.56	0.55	4.71	13.26	0.52	4.54	13.05	0.50	4.50	12.94	0.49	4.44	12.93
		RMSE	0.67	6.15	17.05	0.65	5.92	16.71	0.61	5.79	16.53	0.59	5.73	16.44	0.58	5.68	16.36
	Boulder	MAE	0.51	1.31	4.05	0.39	1.08	3.65	0.37	0.99	3.48	0.32	0.93	3.41	0.30	0.90	3.23
		RMSE	<b>0.66</b>	1.60	4.95	<b>0.47</b>	1.32	4.39	<b>0.43</b>	1.18	4.10	<b>0.38</b>	1.11	3.99	<b>0.35</b>	1.05	3.79
	Dundee	MAE	0.74	1.76	<b>23.94</b>	0.71	1.70	<b>23.05</b>	0.68	1.65	<b>21.92</b>	0.65	1.62	<b>21.54</b>	<b>0.64</b>	1.60	<b>21.48</b>
		RMSE	0.94	2.09	<b>29.59</b>	0.89	2.01	<b>28.92</b>	0.83	1.91	<b>27.91</b>	0.81	1.87	<b>27.10</b>	0.80	1.86	<b>27.56</b>
	Perth	MAE	<b>0.89</b>	<b>2.01</b>	<b>18.20</b>	<b>0.76</b>	<b>1.74</b>	<b>16.82</b>	<b>0.70</b>	<b>1.62</b>	<b>16.01</b>	<b>0.67</b>	<b>1.55</b>	<b>15.16</b>	<b>0.60</b>	<b>1.41</b>	<b>14.12</b>
		RMSE	<b>1.09</b>	<b>2.38</b>	23.28	<b>0.92</b>	<b>2.10</b>	22.01	<b>0.84</b>	<b>1.97</b>	21.06	<b>0.80</b>	1.91	20.62	<b>0.74</b>	<b>1.76</b>	19.00
LSTM	Palo Alto	MAE	<b>0.55</b>	<b>4.44</b>	11.93	<b>0.52</b>	<b>4.21</b>	11.61	<b>0.49</b>	<b>4.02</b>	11.39	<b>0.47</b>	<b>3.97</b>	11.31	<b>0.46</b>	<b>3.91</b>	11.27
		RMSE	<b>0.65</b>	<b>5.68</b>	<b>15.62</b>	<b>0.62</b>	<b>5.43</b>	<b>15.27</b>	<b>0.58</b>	<b>5.28</b>	<b>15.08</b>	<b>0.56</b>	<b>5.22</b>	<b>14.99</b>	<b>0.55</b>	<b>5.17</b>	<b>14.90</b>
	Boulder	MAE	0.58	1.57	5.79	0.46	1.40	5.58	0.43	1.33	5.52	0.39	1.28	5.52	0.36	1.24	5.49
		RMSE	0.71	1.84	6.63	0.53	1.60	6.28	0.49	1.49	6.10	0.44	1.44	6.05	0.42	1.38	5.93
	Dundee	MAE	<b>0.72</b>	<b>1.63</b>	28.69	<b>0.69</b>	<b>1.57</b>	28.32	<b>0.66</b>	<b>1.53</b>	27.32	<b>0.64</b>	<b>1.49</b>	26.12	<b>0.64</b>	<b>1.48</b>	26.86
		RMSE	<b>0.88</b>	<b>1.89</b>	31.21	<b>0.83</b>	<b>1.80</b>	30.57	<b>0.77</b>	<b>1.71</b>	29.75	<b>0.75</b>	<b>1.67</b>	28.70	<b>0.75</b>	<b>1.67</b>	29.30
	Perth	MAE	0.94	2.10	18.33	0.80	1.83	16.95	0.74	1.71	16.37	0.71	1.64	15.56	0.65	1.52	14.93
		RMSE	1.12	2.50	25.06	0.96	2.24	23.86	0.89	2.11	23.03	0.85	2.05	22.62	0.79	1.92	21.15
Transformer	Palo Alto	MAE	0.57	4.89	<b>11.59</b>	0.55	4.68	<b>11.11</b>	0.52	4.55	<b>10.83</b>	0.51	4.50	<b>10.70</b>	0.50	4.46	<b>10.62</b>
		RMSE	0.70	6.47	16.36	0.68	6.24	16.01	0.65	6.11	15.81	0.63	6.05	15.71	0.62	6.00	15.61
	Boulder	MAE	<b>0.45</b>	<b>1.14</b>	<b>3.47</b>	<b>0.35</b>	<b>0.98</b>	<b>3.14</b>	<b>0.35</b>	<b>0.88</b>	<b>2.89</b>	<b>0.31</b>	<b>0.83</b>	<b>2.81</b>	<b>0.28</b>	<b>0.77</b>	<b>2.63</b>
		RMSE	0.67	<b>1.54</b>	<b>4.49</b>	<b>0.47</b>	<b>1.27</b>	<b>4.00</b>	0.44	<b>1.13</b>	<b>3.62</b>	0.39	<b>1.06</b>	<b>3.54</b>	0.36	<b>0.98</b>	<b>3.25</b>
	Dundee	MAE	1.84	4.07	93.57	1.82	4.03	93.34	1.82	4.05	94.51	1.79	3.99	93.05	1.79	3.98	93.05
		RMSE	2.17	4.65	107.40	2.13	4.60	107.13	2.10	4.57	107.66	2.09	4.53	106.56	2.07	4.52	106.48
	Perth	MAE	0.96	2.12	19.21	0.83	1.85	17.81	0.77	1.73	17.27	0.73	1.67	16.64	0.67	1.53	15.76
		RMSE	1.13	2.49	25.21	0.97	2.23	24.01	0.90	2.11	23.22	0.86	2.05	22.83	0.80	1.91	21.36

horizons, with station-level MAE values around 0.21, compared to 0.26 for ARIMA. Similarly, in Dundee, Transformers dominate regional- and city-level forecasts, while ARIMA attains the lowest station-level MAE but is outperformed by Transformers in terms of RMSE. In Palo Alto, Transformers consistently yield the lowest errors at regional and city scales, whereas XGBoost achieves the best station-level performance, with MAE and RMSE values of approximately 0.87 and 1.01, respectively. Overall, Transformer models emerge as the most reliable short-term forecasting approach across datasets, particularly at regional and city aggregation levels. LSTM exhibits strong dataset-specific performance in Perth, while XGBoost demonstrates competitive behavior only in localized station-level forecasting. ARIMA and GRU generally deliver intermediate performance and do not consistently outperform deep learning models in short-term scenarios.

Moving to the mid-term horizon (up to 8 hours, in 2-hour steps, as shown in Table 3), a clearer separation between model families is revealed, while a dataset-dependent behavior is still exhibited. GRU achieves the lowest errors consistently in the Dundee and Perth datasets across all mid-term horizons and spatial aggregation levels, indicating strong robustness in these two cities. In Palo Alto, Transformer models dominate the aggregated forecasts, achieving the best performance at both regional and city scales across 2–8 hour horizons (e.g., city-level MAE decreases from 6.02 at 2 hours to 4.99 at 8 hours). In Boulder, ARIMA performs best at the station and regional levels for most mid-term horizons, whereas LSTM achieves the lowest errors at the city level across the same horizons (e.g., city MAE decreases from 2.91 at 2 hours to 2.39 at 8 hours). XGBoost remains competitive only in selected localized settings, most notably at the Palo Alto station level, where it attains the lowest RMSE, while underperforming at higher aggregation levels and in the remaining datasets. Across datasets, errors generally decrease as the forecasting horizon increases. Although this may appear counter-intuitive, this behavior is well documented in load forecasting under temporal aggregation: short-term EV charging demand is highly volatile, whereas longer horizons smooth out noise and reveal more regular patterns that models can capture more reliably [8].

As for the long-term forecasting (up to 5 days, in 1-day steps, as represented in Table 4), performance is strongly influenced by both dataset characteristics and spatial aggregation level. In Boulder, Transformer models achieve the lowest MAE across all spatial levels and horizons (e.g., city MAE decreases from 3.47 at 1 day to 2.63 at 5 days), indicating strong effectiveness for this dataset. In Palo Alto, LSTM provides the best performance at the station and regional levels across 1–5 days, while at the city level Transformer attains the lowest MAE (e.g., 11.59 at 1 day decreasing to 10.62 at 5 days) and LSTM achieves the lowest RMSE (e.g., 15.62 decreasing to 14.90). In Dundee, a clear divergence is observed: GRU yields the best city-level forecasts (city MAE around 23.94 at 1 day and 21.48 at 5 days), whereas Transformer performs substantially worse, with city-level errors an order of magnitude higher (city MAE of approximately 93 and RMSE of 106 across horizons). Finally, in Perth, GRU consistently achieves the lowest MAE across station, regional, and city levels, while ARIMA attains the lowest city-level RMSE across all horizons (e.g., 22.00 at 1 day decreasing to 18.60 at 5 days). As in the mid-term case, the general reduction in error with increasing horizon can be attributed to temporal aggregation, which suppresses short-term variability and emphasizes lower-frequency patterns that are more predictable over multi-day horizons.

Overall, the experimental results demonstrate that forecasting performance depends strongly on both the prediction horizon and the spatial aggregation level, with consistent trends observed across datasets alongside meaningful dataset-specific deviations. In short-term forecasting, deep learning models generally outperform classical approaches, with Transformer models performing particularly well at regional and city aggregation levels, while LSTM exhibits strong dataset-specific dominance in Perth. As the forecasting horizon increases, recurrent neural networks emerge as the most reliable

models: GRU and LSTM consistently achieve the lowest errors in mid- and long-term forecasting across most datasets and aggregation levels. Transformer models perform competitively in several settings, particularly under coarser spatial aggregation, but also exhibit pronounced sensitivity to dataset characteristics, including notable performance degradation in the Dundee dataset for long-term forecasting. ARIMA remains competitive in isolated cases but does not scale effectively to longer horizons or higher levels of spatial aggregation, while XGBoost shows limited competitiveness outside specific localized scenarios. Overall, these results indicate that models explicitly designed for sequential learning provide the most robust and reliable performance for EV charging load forecasting across diverse temporal and spatial contexts.

## 5 RELATED WORK

This section reviews related work on EV charging load forecasting. We first summarize the broader landscape of forecasting models that have been applied in this domain, highlighting the range of methodological approaches and typical forecasting horizons used in prior studies. We then discuss studies that conduct direct model comparisons and are therefore more closely related to our work.

Traditional models such as ARIMA and SARIMA perform adequately under stable, linear assumptions but struggle with the irregularity of EV charging behavior. For instance, Louie [17] applied SARIMA to Washington and San Diego station data, achieving reasonable seasonal modeling but with declining accuracy at longer horizons. Machine learning approaches, particularly Random Forests and gradient boosting, often outperform statistical methods in short-term forecasting. Lu et al. [18] showed that Random Forests effectively captured Shenzhen station consumption patterns, while CatBoost has demonstrated competitive results for daily EV load forecasting, albeit with challenges in interpretability and hyperparameter tuning. Deep learning methods, notably LSTM and GRU, have shown clear advantages. Zhu et al. [19] reported a 30% reduction in error using LSTM compared to ANN on Shenzhen data. Unterluggauer et al. [20] highlighted the effectiveness of LSTMs for multi-step forecasting in Finland, while Ma and Faye [21] achieved near-perfect short-term accuracy with LSTMs. More recent studies integrate spatial features into the forecasting process. Adinkrah et al. [22] reviewed AI-based methods combining clustering with time series forecasting, while Hüttel et al. [23] employed Temporal Graph Convolutional Networks (TGCN) to exploit spatial adjacency. Zhang et al. [24] further advanced this line of work by applying Graph Neural Networks (GNNs) for hourly station-level forecasting, surpassing traditional baselines. Transformers have also gained traction in this domain. Koohfar et al. [6] applied Transformer architectures to five years of Boulder station data across horizons from 7 to 90 days, consistently outperforming ARIMA, RNN, and LSTM models.

Beyond methodological proposals, a smaller but growing body of research has focused on experimental comparisons of forecasting models for EV charging. Unlike studies that introduce a single new algorithm, these works benchmark multiple methods under common settings, making them directly comparable to our approach. Reviewing these efforts highlights both their contributions and the distinctive aspects of our study.

**Hybrid Prophet–LSTM models.** Wei et al. [25] investigate load forecasting for a charging station in southern China using a hybrid model that combines Prophet with LSTM, optimized through a genetic algorithm (GA). Their evaluation, based on daily station-level demand, compares their approach against ARIMA, Prophet, and LSTM baselines. Results show that GA-Prophet-LSTM consistently outperforms the individual models in terms of RMSE and MAPE. While this work provides a clear comparative evaluation, it is limited to a single dataset and daily granularity. In contrast, our study broadens the scope by considering multiple cities, finer temporal resolutions,

and spatial aggregation levels.

**Global versus local forecasting models.** Van Etten et al. [26] propose a large-scale framework for EV charging demand forecasting using *global* models trained across multiple stations. Their study evaluates ARIMA, Transformers, and the N-HiTS architecture on four datasets (London, Palo Alto, Perth, Boulder), using daily horizons of 1, 7, and 30 days. A key novelty lies in testing generalization, where models trained on one set of stations are applied to unseen stations in other regions. Compared to our work, their analysis emphasizes transferability across locations, while ours emphasizes scalability across horizons and spatial aggregation levels (station, region, city). Moreover, their evaluation is restricted to daily data, whereas we include 10-minute, hourly, and daily resolutions. Together, these studies are complementary: their study highlights the potential of global training for cross-station generalization, while our study provides a benchmark across temporal and spatial scales.

**Real-time availability forecasting.** Manai et al. [27] address the related problem of real-time station availability prediction. Using large-scale datasets from Paris (Belib API) and Estonia (Enefit VOLT), they evaluate models including KNN, logistic regression, Random Forest, SVM, and an Artificial Neural Network (ANN). They also propose an ensemble combining ANN and RF, which outperforms individual baselines across precision, recall, and F1-score. While this study shares our comparative orientation and use of diverse real-world datasets, its target variable differs: station availability (*classification*) rather than energy consumption (*regression*). Moreover, their emphasis is on station-level, user-facing predictions, while our study focuses on multi-horizon load forecasting for infrastructure and grid planning.

**Forecasting with contextual features.** Mystakidis et al. [28] present a forecasting framework that integrates traffic flow, weather conditions, and user charging behavior to predict hourly EV demand at a residential complex in Trondheim, Norway. To address zero-inflated demand patterns, they introduce a Logarithmic Zero-Inflated (LogZI) regression method, achieving substantial improvements over conventional models in  $R^2$ , MAE, and RMSE. While their work demonstrates the benefits of incorporating exogenous information and specialized regression techniques, its scope is narrower: one-step-ahead hourly forecasts at a single site. In contrast, our study deliberately restricts to historical load and calendar features, enabling a controlled comparison of model families across multiple horizons and aggregation levels.

To illustrate the heterogeneity of related work, Table 5 categorizes the studies reviewed in this section with respect to the models used and prediction settings. It is clear that most prior work focuses on a single forecasting horizon or, at most, a limited subset of horizons, and relies on a single dataset. In contrast, our study evaluates multiple model families across a wide range of forecasting horizons over four benchmark datasets, providing a more comprehensive view of model performance across diverse forecasting scenarios.

## 6 CONCLUSIONS AND FUTURE WORK

### 6.1 Summary and Contributions

This study conducted a systematic experimental comparison of time series forecasting methods for EV charging demand across different temporal and spatial horizons. Forecasts were evaluated at short-term (up to 30 minutes), mid-term (up to 8 hours), and long-term (up to 5 days) horizons, and at three spatial aggregation levels ranging from individual charging stations to regional and city-wide demand.

The analysis was based on four publicly available real-world datasets with diverse characteristics. Five forecasting approaches were benchmarked: a classical statistical model (ARIMA), a machine

Table 5: Summary of Key Studies on EV Charging Consumption Forecasting

Study	Model(s) evaluated	Dataset	Forecasting Horizon		
			Short-term (minutes)	Mid-term (hours)	Long-term (days)
<b>Our study</b>	<b>ARIMA, XGBoost, GRU, LSTM, Transformer</b>	<b>Palo Alto (USA), Boulder (USA), Dundee (UK), Perth (Australia)</b>	<b>10, 20, 30</b>	<b>2, 4, 6, 8</b>	<b>1, 2, 3, 4, 5</b>
Louie [17]	SARIMA	San Diego (USA)	–	–	1
Lu et al. [18]	Random Forests	Shenzhen (China)	15	–	1
Zhu et al. [19]	LSTM, GRU, ANN	Shenzhen (China)	60	–	–
Unterluggauer et al. [20]	Multivariate LSTM	Austria	60	–	1
Ma & Faye [21]	LSTM	Dundee (UK)	10	6	–
Hüttel et al. [23]	TGCN	Palo Alto (USA)	–	–	1, 7, 30
Zhang et al. [24]	GNN	Unspecified	15, 30, 60	–	–
Koohfar et al. [6]	Transformer, ARIMA, LSTM, GRU	Boulder (USA)	–	–	7, 30, 60, 90
Wei et al. [25]	ARIMA, Prophet, LSTM, GA-Prophet-LSTM	China	–	–	1
Van Etten et al. [26]	N-HiTS (global), N-HiTS (local), Transformer, ARIMA, Naive	London (UK), Palo Alto (USA), Perth (Scotland), Boulder (USA)	–	–	1, 7, 30
Mystakidis et al. [28]	ZI / LogZI regression; XGBR, LGBMR, HGBR, CBR, RFR, SVR, LSTM, GRU, MLP	Trondheim (Norway)	60	–	–

learning model (XGBoost), and three deep learning architectures (GRU, LSTM, and Transformer). All models were trained and evaluated within a unified experimental pipeline, and performance was assessed using MAE and RMSE across identical temporal horizons and spatial aggregation levels.

The results reveal clear differences across model families and forecasting scenarios. Transformer models are particularly effective in short-term forecasting, especially at regional and city aggregation levels, where they frequently achieve the lowest errors across datasets. ARIMA remains competitive only in isolated station-level cases but does not scale reliably as forecasting horizons increase or spatial aggregation becomes coarser. In contrast, GRU and LSTM consistently deliver the most accurate forecasts in mid- and long-term scenarios, particularly at regional and city scales, highlighting their strength in modeling complex sequential dependencies. Transformer models exhibit mixed behavior beyond the short term and do not consistently outperform recurrent architectures in mid- and long-term forecasting, indicating sensitivity to dataset characteristics and model configuration. XGBoost achieves competitive performance in selected localized scenarios but generally underperforms at higher levels of spatial aggregation.

By systematically evaluating multiple model families across a wide range of temporal horizons and spatial resolutions, this study provides a comprehensive and reproducible benchmark for EV charging load forecasting. The findings highlight important trade-offs between statistical, machine learning, and deep learning approaches, and underscore the importance of selecting forecasting models that are well matched to the temporal and spatial requirements of the target application.

## 6.2 Future Work

Several directions remain open for future research. First, while fixed configurations were used to ensure comparability, further improvements could be achieved through systematic hyperparameter optimization and exploration of deeper or more specialized architectures.

Second, the study focused exclusively on historical load and calendar-based features. Incorporating exogenous variables, such as: weather, traffic patterns, electricity prices, or station location characteristics, may improve explanatory power and predictive accuracy.

Finally, to better understand generalization and reduce data requirements, future research could explore eXplainable AI (XAI) and transfer learning techniques. These would, on the one hand, provide insights into the main parameters that affect each model’s prediction quality, and, on the other, allow knowledge gained from forecasting in one city’s charging stations to be applied to another, potentially improving scalability and adaptability across regions.

## Acknowledgment

This work was supported in part by the Horizon Europe Research and Innovation Programme of the European Union under grant agreement No. 101070416 (Green.Dat.AI; <https://greendatai.eu>) and in part by the University of Piraeus Research Center.

## References

- [1] International Energy Agency (IEA), *Global EV Outlook 2023: Catching up with climate ambitions*, Paris, France: IEA, 2023. [Online]. Available: <https://www.iea.org/reports/global-ev-outlook-2023>
- [2] United Nations Framework Convention on Climate Change (UNFCCC), *The Paris Agreement*, Dec. 2015. [Online]. Available: <https://unfccc.int/process-and-meetings/the-paris-agreement>

- [3] S. Sanami, H. Mosalli, Y. Yang, H.-G. Yeh, and A. G. Aghdam, "Demand forecasting for electric vehicle charging stations using multivariate time-series analysis," *arXiv preprint arXiv:2502.16365*, 2025. [Online]. Available: <https://arxiv.org/abs/2502.16365>
- [4] V. S. M. Babu K., P. Chakraborty, and M. Pal, "Planning of fast charging infrastructure for electric vehicles in a distribution system and prediction of dynamic price," *Int. J. Electr. Power Energy Syst.*, vol. 155, p. 109502, 2024. [Online]. Available: <https://doi.org/10.1016/j.ijepes.2023.109502>
- [5] M. Yilmaz and P. T. Krein, "Review of battery charger topologies, charging power levels and infrastructure for plug-in electric and hybrid vehicles," *IEEE Trans. Power Electron.*, vol. 28, no. 5, pp. 2151–2169, May 2013. [Online]. Available: <https://doi.org/10.1109/TPEL.2012.2212917>
- [6] S. Koochfar, W. Woldemariam, and A. Kumar, "Prediction of electric vehicles charging demand: A transformer-based deep learning approach," *Sustainability*, vol. 15, no. 3, p. 2105, 2023. [Online]. Available: <https://doi.org/10.3390/su15032105>
- [7] M. Yilmaz and P. T. Krein, "Review of the impact of vehicle-to-grid technologies on distribution systems and utility interfaces," *IEEE Trans. Power Electron.*, vol. 28, no. 12, pp. 5673–5689, Dec. 2013, doi: 10.1109/TPEL.2012.2227500
- [8] R. J. Hyndman and G. Athanasopoulos, *Forecasting: Principles and Practice*, 3rd ed., Melbourne, Australia: OTexts, 2021. [Online]. Available: <https://otexts.com/fpp3>
- [9] G. E. P. Box, G. M. Jenkins, G. C. Reinsel, and G. M. Ljung, *Time Series Analysis: Forecasting and Control*, 5th ed. Hoboken, NJ, USA: Wiley, 2015. [Online]. Available: <https://www.wiley.com/en-us/Time-Series-Analysis-Forecasting-and-Control-5th-Edition-p-9781118675021>
- [10] T. Chen and C. Guestrin, "XGBoost: A scalable tree boosting system," in *Proc. 22nd ACM SIGKDD Int. Conf. Knowl. Discovery Data Mining (KDD)*, San Francisco, CA, USA, 2016, pp. 785–794. [Online]. Available: <https://doi.org/10.1145/2939672.2939785>
- [11] K. Cho, B. van Merriënboer, C. Gulcehre, *et al.*, "Learning phrase representations using RNN encoder–decoder for statistical machine translation," *arXiv preprint arXiv:1406.1078*, 2014. [Online]. Available: <https://arxiv.org/abs/1406.1078>
- [12] S. Hochreiter and J. Schmidhuber, "Long short-term memory," *Neural Comput.*, vol. 9, no. 8, pp. 1735–1780, 1997. [Online]. Available: <https://doi.org/10.1162/neco.1997.9.8.1735>
- [13] A. Vaswani, N. Shazeer, N. Parmar, *et al.*, "Attention is all you need," in *Proc. Adv. Neural Inf. Process. Syst. (NeurIPS)*, Long Beach, CA, USA, 2017, pp. 5998–6008. [Online]. Available: <https://arxiv.org/abs/1706.03762>
- [14] Y. Amara, "EV load open data," GitHub repository, 2023. [Online]. Available: <https://github.com/yvenn-amara/ev-load-open-data>
- [15] S. Makridakis, S. C. Wheelwright, and R. J. Hyndman, *Forecasting: Methods and Applications*, 3rd ed., Hoboken, NJ, USA: Wiley, 1998. [Online]. Available: <https://hephaestus.nup.ac.cy/handle/11728/7113>

- [16] S. P. Shakti, M. K. Hassan, Y. Zhenning, *et al.*, "Annual automobile sales prediction using ARIMA model," *Int. J. Hybrid Inf. Technol.*, vol. 10, no. 6, pp. 13–22, 2017. [Online]. Available: <https://doi.org/10.14257/ijhit.2017.10.6.02>
- [17] H. M. Louie, "Time-series modeling of aggregated electric vehicle charging station load," *Electr. Power Compon. Syst.*, vol. 45, no. 14, pp. 1498–1511, 2017. [Online]. Available: <https://doi.org/10.1080/15325008.2017.1336583>
- [18] Y. Lu, Y. Li, D. Xie, *et al.*, "The application of improved random forest algorithm on the prediction of electric vehicle charging load," *Energies*, vol. 11, no. 11, p. 3207, 2018. [Online]. Available: <https://doi.org/10.3390/en11113207>
- [19] J. Zhu, Z. Yang, Y. Guo, *et al.*, "Short-term load forecasting for electric vehicle charging stations based on deep learning approaches," *Appl. Sci.*, vol. 9, no. 9, p. 1723, 2019. [Online]. Available: <https://doi.org/10.3390/app9091723>
- [20] T. Unterluggauer, K. Rauma, P. Järventausta, and C. Rehtanz, "Short-term load forecasting at electric vehicle charging sites using a multivariate multi-step long short-term memory: A case study from Finland," *IET Electr. Syst. Transp.*, vol. 11, no. 4, pp. 405–419, 2021. [Online]. Available: <https://doi.org/10.1049/els2.12028>
- [21] T.-Y. Ma and S. Faye, "Multistep electric vehicle charging station occupancy prediction using hybrid LSTM neural networks," *arXiv preprint arXiv:2106.04986*, Jun. 2021, revised Nov. 2021. [Online]. Available: <https://doi.org/10.48550/arXiv.2106.04986>
- [22] J. Adinkrah, F. Kemausuor, E. T. Tchao, *et al.*, "Artificial intelligence-based strategies for sustainable energy planning and electricity demand estimation: A systematic review," *Renew. Sustain. Energy Rev.*, vol. 210, p. 115161, 2025. [Online]. Available: <https://doi.org/10.1016/j.rser.2024.115161>
- [23] F. B. Hüttel, I. Peled, and F. C. Pereira, "Deep spatio-temporal forecasting of electric vehicle charging demand," *arXiv preprint arXiv:2106.10940*, Jun. 2021. [Online]. Available: <https://arxiv.org/abs/2106.10940>
- [24] Z. Zhang, C. Liu, X. Rao, *et al.*, "Spatial-temporal load forecasting of electric vehicle charging stations based on graph neural network," *J. Intell. Fuzzy Syst.*, vol. 46, no. 4, pp. 1–16, 2024. [Online]. Available: <https://doi.org/10.3390/en17194798>
- [25] Y. Wei, Y. Jiang, J. Song, Z. Sheng, X. Song, *et al.*, "Load forecasting of battery electric vehicle charging station based on GA-Prophet-LSTM," *J. Phys.: Conf. Ser.*, vol. 2592, 012092, 2023. [Online]. Available: <https://doi.org/10.1088/1742-6596/2592/1/012092>
- [26] T. van Etten, V. Degeler, and D. Luo, "Large-scale forecasting of electric vehicle charging demand using global time series modeling," in *Proc. 10th Int. Conf. Vehicle Technol. Intell. Transp. Syst. (VEHITS)*, SciTePress, 2024, pp. 40–51. [Online]. Available: <https://doi.org/10.5220/0012555400003702>
- [27] M. Manai, B. Sellami, and S. Ben Yahia, "Towards a smarter charging infrastructure: Real-time availability forecasting for EVs," *Procedia Comput. Sci.*, vol. 246, pp. 930–939, 2024. [Online]. Available: <https://doi.org/10.1016/j.procs.2024.09.512>

- [28] A. Mystakidis, N. Tsalikidis, P. Koukaras, et al., "EV charging forecasting exploiting traffic, weather and user information," *Int. J. Mach. Learn. Cybern.*, vol. 16, pp. 6737–6763, 2025. [Online]. Available: <https://doi.org/10.1007/s13042-025-02643-8>